Eur. Phys. J. C (2023) 83:629
https://doi.org/10.1140/epjc/s10052-023-11634-4

THE EUROPEAN PHYSICAL JOURNAL C

Regular Article - Experimental Physics

Measurement of $\tau_{\rm L}$ using the $B_s^0 \to J/\psi\eta$ decay mode

LHCb collaboration[⋆]

CERN, 1211 Geneva 23, Switzerland

Received: 8 June 2022 / Accepted: 2 October 2022

Abstract Using a proton–proton collision data sample collected by the LHCb detector and corresponding to an integrated luminosity of 5.7 fb^{-1}, the lifetime of the light B_s^0 mass eigenstate, τ_L, is measured using the $B_s^0 \to J/\psi\eta$ decay mode to be

$$\tau_{\rm L} = 1.445 \pm 0.016({\rm stat}) \pm 0.008({\rm syst})\,{\rm ps}.$$

A combination of this result with a previous LHCb analysis using an independent dataset corresponding to 3 fb^{-1} of integrated luminosity gives

$$\tau_{\rm L} = 1.452 \pm 0.014 \pm 0.007 \pm 0.002\,{\rm ps},$$

where the first uncertainty is statistical, the second due to the uncorrelated part of the systematic uncertainty and the third due to the correlated part of the systematic uncertainty.

1 Introduction

In the Standard Model (SM), the B_s^0 and $\overline{B}_s^0$ flavour eigenstates can be expressed as a linear combination of the heavy (H) and light (L) mass eigenstates with decay widths $\Gamma_{\rm H}$ and $\Gamma_{\rm L}$, respectively. A sizeable difference between these decay widths is predicted [1]. The effective lifetime of a B_s^0 meson in a specific decay mode is measured by fitting the decay time distribution with a single exponential function [2,3]. The experimental data on the weak mixing phase, ϕ_s, are consistent with the SM prediction that CP violation in $B_s^0 - \overline{B}_s^0$ mixing is small [1]. Consequently, the mass eigenstates are also CP eigenstates to better than per mille level and the effective lifetime measured in $B_s^0 \to J/\psi\eta$ decays is equal, to good approximation, to $\tau_{\rm L} = 1/\Gamma_{\rm L}$. Using the SM prediction for $\Delta\Gamma_s$ from Ref. [1], and the value of $\tau_{B_s^0}/\tau_{B^0}$ given in Ref. [4], together with the measured lifetime of the B^0 meson [5] gives τ_L =1.422 ± 0.013 ps. Measurements of $\tau_{\rm L}$ have been reported by the LHCb collaboration using the tree-level decay modes $B_s^0 \to J/\psi\eta$ [6], $B_s^0 \to D_s^+ D_s^-$ [7] and the loop dominated $B_s^0 \to K^+K^-$ [8] where hadronic uncertainties are more important. These measurements use data collected during Run 1 of the LHC at centre-of-mass energies, $\sqrt{s} = 7$ and 8 TeV, corresponding to an integrated luminosity of 3 fb^{-1}. The lifetime of the heavy mass eigenstate, $\tau_{\rm H}$, has been measured using the $B_s^0 \to J/\psi\, f_0(980)$ mode [9–11]. Improving the precision of $\tau_{\rm L}$ and $\tau_{\rm H}$ enables more stringent tests of the consistency between direct measurements of the decay-width difference, $\Delta\Gamma_s = \Gamma_{\rm L} - \Gamma_{\rm H}$, in $B_s^0 \to J/\psi\phi$ decays and those inferred from effective lifetimes.

In this paper, $\tau_{\rm L}$ is measured in the $B_s^0 \to J/\psi\eta$ decay mode using a data sample, corresponding to an integrated luminosity of 5.7 fb^{-1}, collected in proton–proton (pp) collisions at $\sqrt{s} = 13$ TeV during Run 2 of the LHC (2015–2018). The analysis builds on the Run 1 study described in Ref. [6] which used around 3 fb^{-1} collected at $\sqrt{s} = 7, 8$ TeV. The J/ψ meson is reconstructed via the dimuon decay mode and the η meson through its decay to a pair of photons.

2 Detector and simulation

The LHCb detector [12,13] is a single-arm forward spectrometer covering the pseudorapidity range $2 < \eta < 5$, designed for the study of particles containing b or c quarks. It includes a high-precision tracking system consisting of a silicon-strip vertex detector (VELO) surrounding the pp interaction region, a large-area silicon-strip detector (TT) located upstream of a dipole magnet with a bending power of approximately 4 Tm, and three stations of silicon-strip detectors and straw drift tubes placed downstream of the magnet. The tracking system provides a measurement of the momentum, p, of charged particles with a relative uncertainty that varies from 0.5 % at low momentum to 1.0 % at 200 GeV/c. Large samples of $J/\psi \to \mu^+\mu^-$ and $B^+ \to J/\psi K^+$ decays, collected concurrently with the data set used here, were used to calibrate the momentum scale of the spectrometer using the procedure discussed in Ref. [14]. The relative accuracy of this procedure is determined using samples of other fully

⋆ e-mail: ozlem.ozcelik@cern.ch

Published online: 17 July 2023

reconstructed b-hadrons and Υ mesons, and is estimated to be 3×10^{-4}. For b-hadron decay modes such $B^+ \to J/\psi K^+$ the mass resolution agrees between data and simulation to better than 10%.

Various charged hadrons are distinguished using information from two ring-imaging Cherenkov detectors. In addition, photons, electrons, and hadrons are identified by a calorimeter system consisting of scintillating-pad and preshower detectors, an electromagnetic and a hadronic calorimeter. The calorimeter response is calibrated using samples of $\pi^0 \to \gamma\gamma$ decays [15]. For this analysis, a further calibration is made using an inclusive sample of $\eta \to \gamma\gamma$ decays, which results in a precision of 0.1 % on the neutral energy scale. The mass resolution on the η meson found in simulation (data) is 22.9 MeV/c^2 (23.9 MeV/c^2). Muons are identified by a system composed of alternating layers of iron and multiwire proportional chambers.

The online event selection is performed by a trigger, which consists of a hardware stage followed by a two-level software stage [16]. An alignment and calibration of the detector is performed in near real-time with the results used in the software trigger [17]. The same alignment and calibration information is propagated to the offline reconstruction, ensuring consistent information between the trigger and offline software. In this analysis, candidate events are required to pass the hardware trigger, which selects muon and dimuon candidates with high transverse momentum, p_{T}, using information from the muon system. The first stage of the software trigger performs a partial event reconstruction and requires events to have two well-identified oppositely charged muons with an invariant mass larger than 2.7 GeV/c^2. The second stage performs a full event reconstruction. Events are retained for further processing if they contain a displaced $J/\psi \to \mu^+\mu^-$ candidate. The decay vertex is required to be well separated from each reconstructed primary vertex (PV) of the proton–proton interaction by requiring the distance between the PV and the J/ψ decay vertex divided by its uncertainty (referred to as the decay-length significance or DLS) to be greater than three. This introduces a non-uniform efficiency for b-hadron candidates that have a decay time less than ~ 0.4 ps.

Simulated pp collisions are generated using Pythia [18,19] with a specific LHCb configuration [20]. Decays of hadronic particles are described by EvtGen [21], in which final-state radiation is generated using Photos [22]. The interaction of the generated particles with the detector, and its response, are implemented using the Geant4 toolkit [23,24] as described in Ref. [25]. Other sources of background, such as those from inclusive $b \to \chi_c$ transitions, where the χ_c decays radiatively to a J/ψ meson, are studied using the RapidSim fast simulation package [26].

3 Selection

As in the LHCb Run 1 analysis of this mode [6], a two-step procedure is used to optimize the selection of $B_s^0 \to J/\psi\eta$ decay candidates. These studies use simulated signal samples together with the high-mass sideband of the data ($5650 < m(J/\psi\eta) < 5850$ MeV/c^2), which is not used in the subsequent determination of τ_{L}. In the first step, loose selection criteria are applied that reduce background significantly whilst retaining high signal efficiency. Subsequently, a multivariate analysis (MVA) is used to reduce further the combinatorial background. This is optimised using pseudoexperiments to obtain the best precision on the measured value of τ_{L}. Compared to the Run 1 analysis, the modifications to both steps improve the signal efficiency and background rejection.

The selection starts with a pair of oppositely charged particles, identified as muons, that form a common decay vertex. To ensure a high efficiency the muon candidates are required to have a pseudorapidity between 2.0 and 4.6. The invariant mass of the dimuon candidate must be within ± 50 MeV/c^2 of the known J/ψ mass [5].

Photons are selected from well-identified neutral clusters reconstructed in the electromagnetic calorimeter [13] that have a transverse energy in excess of 300 MeV. Candidate $\eta \to \gamma\gamma$ decays are selected from diphoton combinations with an invariant mass within 70 MeV/c^2 of the known η mass [5] and with a transverse momentum larger than 2.1 GeV/c.

The J/ψ and η candidates are combined to form candidate B_s^0 mesons, which are required to have p_{T} larger than 2.5 GeV/c. The B_s^0 candidate is assigned to the PV with the smallest χ^2_{IP}, where χ^2_{IP} is defined as the difference in the vertex-fit χ^2 to a given PV reconstructed with and without the candidate being considered. Though lifetime biasing, a loose requirement of $\chi^2_{\mathrm{IP}} < 25$ is applied since it is effective in removing combinatorial background. In addition, to ensure the B_s^0 candidate is matched to the correct PV, if there is another PV for which $\chi^2_{\mathrm{IP}} < 50$ in the event, the candidate is rejected. A kinematic fit is performed to improve the invariant mass resolution [27], where the intermediate resonance masses are constrained to their known values. The χ^2 per degree of freedom of this fit is required to be less than five. The measured decay time of the candidate must be between 0.4 ps and 10 ps. These requirements define a time range where the acceptance is reasonably uniform.

The second step of the selection process is based on a Multilayer Perceptron neural network [28], which is trained using the simulated signal sample and the high-mass sideband of the data for background. Fourteen variables, chosen as they give good separation between signal and background, are used as input to the neural network. It has been checked that these variables are well modelled by the simulation using the $B_s^0 \to J/\psi\eta$ signal after the preselection and subtracting

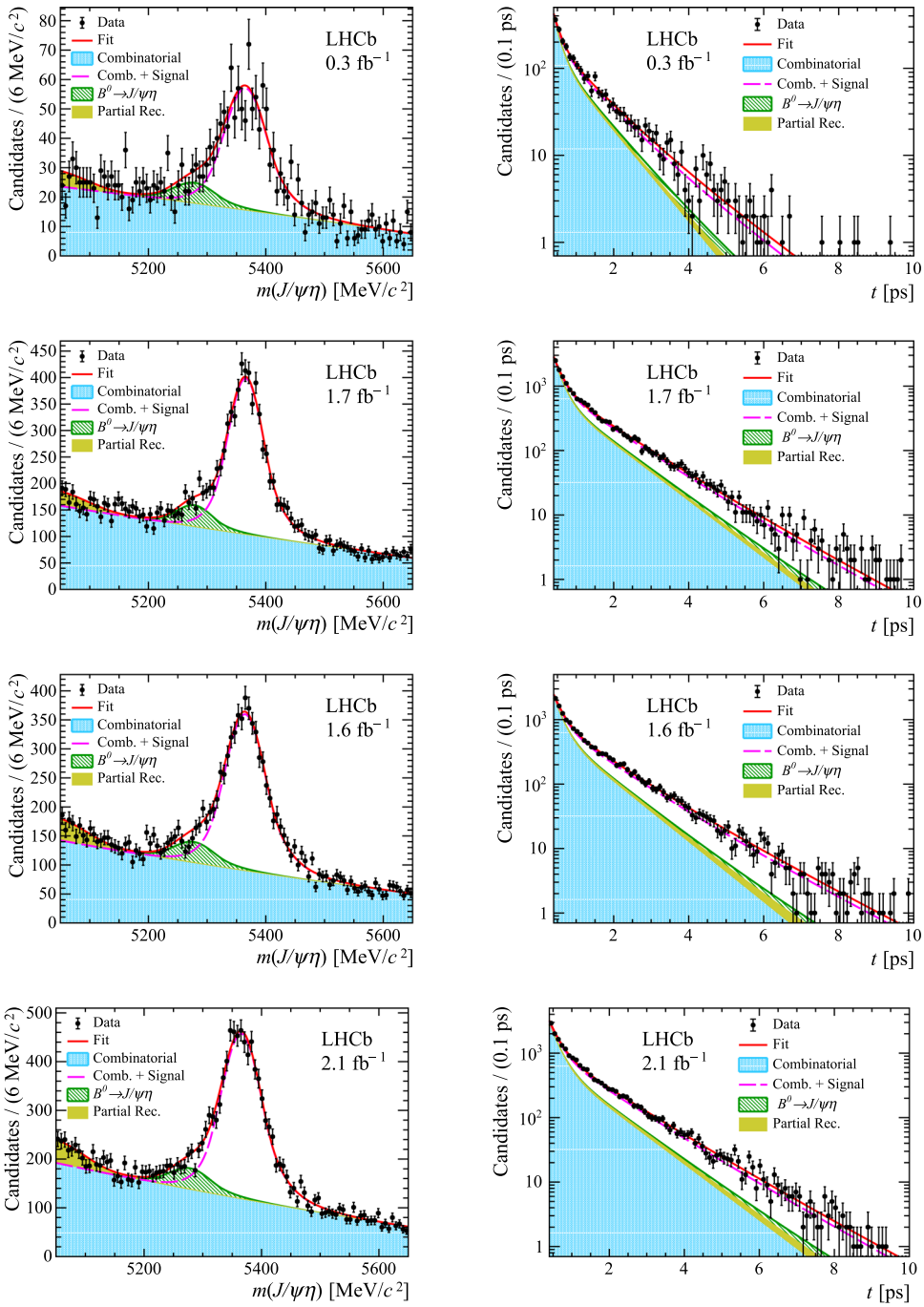

Fig. 1 Distributions of (left) invariant mass and (right) decay time by year: (top row) 2015, (second row) 2016, (third row) 2017 and (bottom row) 2018

the background with the *sPlot* [29] technique and also with the $B^+ \to J/\psi K^+$ control channel.

These are chosen as they give good separation between signal and background, and are known to be well modelled by the simulation. The variables include information on the candidate kinematics, particle identification, vertexing and track quality. An important change compared to the Run 1 analysis is the addition of information related to the isolation of the b-hadron candidate. This is found to be highly effective at suppressing combinatorial background and compensates for the higher multiplicity in the Run 2 environment.

The requirement on the MVA output was chosen to minimize the expected statistical uncertainty on the fitted value of $\tau_{\rm L}$ using pseudoexperiments. The chosen value removes over 99 % of background candidates whilst retaining over 80 % of simulated signal decays. After applying these requirements 5 % of events contain multiple candidates from which only one, chosen at random, is kept.

4 Fit model

Figure 1 shows the $J/\psi\eta$ invariant mass and decay time distributions along with the fit projections for the four years of running (2015, 2016, 2017 and 2018). The value of $\tau_{\rm L}$ is determined from a two-dimensional unbinned maximum likelihood fit to the distributions of the $B^0_{(s)}$ candidate invariant mass, m and decay time. To allow for variations in running conditions, the dataset is divided into the four years of running which are fitted simultaneously. The fit is performed for candidates with $5050 < m(J/\psi\eta) < 5650\,\text{MeV}/c^2$ and $0.4 < t < 10\,\text{ps}$. The fit model has five components: the $B^0_s \to J/\psi\eta$ signal, the $B^0 \to J/\psi\eta$ decay, partially reconstructed $B^0_s \to \chi_{c1,c2}\eta$ decays with the subsequent decay $\chi_c \to J/\psi\gamma$, partially reconstructed $B^0_s \to J/\psi\phi$ with $\phi \to \eta\gamma$ and combinatorial background.

To account for the detector resolution, the decay time distribution of each component is convolved with a Gaussian function with a width of 52 fs determined using the simulation. The variation of the detector efficiency as a function of decay time for each year of running is accounted for by an acceptance function, $A_{\rm tot}$. This is expressed as the product of four components. Firstly, the reconstruction efficiency of the vertex detector is known to decrease as the distance of closest approach of the decay products to the pp beam-line increases [6,30]. This effect is parameterised with a second order polynomial. Improvements in the track reconstruction used in Run 2 led to a reduction for this effect by a factor of three compared to the Run 1 analysis [16]. It is further reduced by the choice of the pseudorapidity range for the muons and cross-checked with the $B^+ \to J/\psi K^+$ decay mode. Secondly, the requirement on the DLS applied in the trigger leads to inefficiency at small proper times. Its effect is minimised by the requirement of $t > 0.4$ ps. The residual effect of this requirement, $A_{\rm DLS}$, is modelled using the simulation and calibrated in data using a large sample of $B^+ \to J/\psi K^+$ decays. Furthermore, the requirement on the B^0_s candidate $\chi^2_{\rm IP}$ leads to an efficiency, $A_{{\rm IP}\chi^2}$, that decreases linearly at higher time. This component is parameterised using simulated signal decays. Finally, the inclusion of the B^0_s candidate $\chi^2_{\rm IP}$ in the MVA leads to a linear acceptance correction ($A_{\rm MVA}$) which is determined using the simulation.

Figure 2 shows the overall acceptance curve, $A_{\rm tot} = A_{\rm VELO} \cdot A_{\rm DLS} \cdot A_{{\rm IP}\chi^2} \cdot A_{\rm MVA}$ obtained for the 2016 dataset. If the data were not corrected for the acceptance, then the bias on $\tau_{\rm L}$, evaluated by fitting the simulated data with and without the correction, would be 18 fs. Different, but qualitatively similar, decay time acceptance curves are evaluated for each year and used in the decay time fit.

The invariant mass distribution for the $B^0_s \to J/\psi\eta$ signal is parameterised by a Double Sided Crystal Ball (DSCB) function. This is a generalization of the Crystal Ball function with power law tails on both sides of the mass peak [31]. Alternative parametrisations including the Bukin function [32] and a skewed Student's t-distribution [33,34] are considered as systematic variations. In the fit to the data, the tail parameters of the DSCB distribution are fixed to the values obtained from simulation, while the mean and width parameter are freely varied in the fit. The decay time distribution for the signal component is modelled with an exponential function convolved with the detector resolution and multiplied by the detector acceptance, as discussed above.

The second component in the fit accounts for the $B^0 \to J/\psi\eta$ decay. Since the invariant mass resolution is approximately $36\,\text{MeV}/c^2$, this component partially overlaps with the B^0_s signal mode. The same DSCB mass shape as for the B^0_s signal decay is used to model this contribution, with a constraint on the mass resolution between the modes, as obtained from simulation. In the fit, the difference between the positions of the B^0_s and B^0 mass peaks is Gaussian-constrained to the known value $M(B^0_s) - M(B^0) = 87.22 \pm 0.16\,\text{MeV}/c^2$ [5]. The decay time of the B^0 component is modelled with an exponential convolved with the same acceptance function and detector resolution as for the B^0_s component. The lifetime is Gaussian-constrained to the known value, $\tau(B^0) = 1.519 \pm 0.005$ ps [5]. Finally, the yield of this component is parameterised as the product of the B^0_s yield for each year multiplied by a common factor between the years, f_r, which is left free. The shape of the combinatorial background in mass and time is studied using the high-mass sideband and mixing samples of J/ψ and η mesons selected in data. Based upon these studies this component is modelled by a second-order Chebyshev polynomial in mass and the sum of two exponentials in decay time.

The RapidSim [26] package is used to study backgrounds from partially reconstructed b-hadron decays and two sources are identified. The first is the decay $B^0_s \to J/\psi\phi$ with the subsequent decay $\phi \to \eta\gamma$. Due to the missing photon, and the mass difference between the ϕ and η mesons, this background has a maximum invariant mass of 5200 MeV/c^2. The shape of this component in mass is modelled with a bifurcated Gaussian function. Its lifetime parameter is Gaussian-constrained to the measured value of the lifetime in the $B^0_s \to J/\psi\phi$ channel, $\tau = 1.480 \pm 0.007$ ps [35] multiplied by a factor of 0.99, determined from the simulation, that accounts for the missing photon energy. The relative yield of this component to the signal is Gaussian-constrained to be $f_\phi = (0.6 \pm 0.1)\%$ using the known branching fractions [5] and the relative efficiency from the simulation. The second source of partially reconstructed background is due to $B^0_s \to \chi_{c1,c2}\eta$ decays. The branching fractions for these decay modes are not measured but the rate for the decay to the χ_{c1} meson is most likely higher than that of the χ_{c2} decay mode from spin suppression arguments. Consequently, the yield of the χ_{c1} component, $N_{\chi_{c1}}$, is left to freely vary in the fit. The yield of the χ_{c2} component is Gaussian-constrained

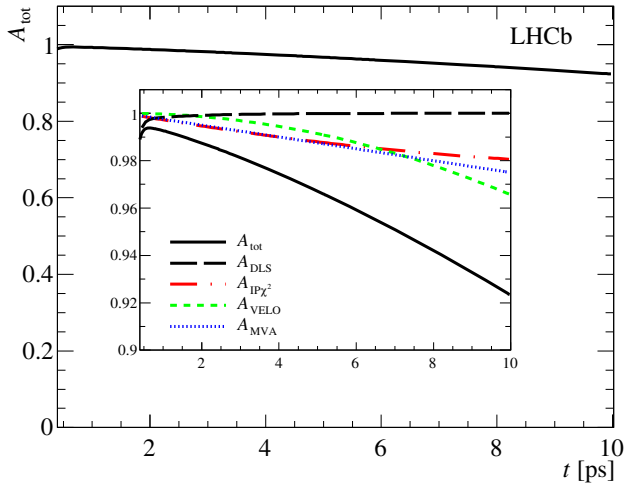

Fig. 2 Total acceptance function, $A_{\rm tot}$ for the 2016 data taking period. The insert shows the four individual components of the acceptance that are multiplied to give $A_{\rm tot}$. The acceptance functions for the other years are similar

to be $f_{\chi c2} N_{\chi c1}$ where $f_{\chi c2} = 0.1 \pm 0.1$ based on the values seen for other decay modes [5]. The shape of these components in mass is modelled by an error function, based on simulation. The unknown lifetime parameter of this component is left free in the fit. The validity of these assumptions is tested as part of the study of systematic uncertainties.

In total the simultaneous fit to the four years of running has 40 free parameters. The correctness of the fit procedure is validated using the full simulation and pseudoexperiments. No significant bias compared to the uncertainty of the measurement is found, and the uncertainties estimated by the fit are found to be accurate.

5 Results and systematic uncertainties

The fit gives a measured lifetime of $\tau_{\rm L} = 1.445 \pm 0.016$ ps. The values of other fitted parameters, such as the mass resolution are in good agreement with the expectation from the simulation. As discussed in Sect. 4, uncertainties on physics parameters are propagated to the statistical uncertainty via Gaussian constraints. The dominant uncertainty arises from the size of the simulation sample used to model the acceptance function. The uncertainty due to each of the individual acceptance corrections is estimated by resampling the covariance matrix of the determined PDF and by changing the functional form used for each component. The check of acceptance shape due to the VELO tracking efficiency using the $B^+ \to J/\psi K^+$ data is limited by the knowledge of the B^+ lifetime giving a further 4 fs uncertainty.

Possible biases from misalignment of the VELO detector halves are evaluated by dividing the data into three categories according to which side of the VELO the tracks traverse and re-running the fit. This gives a systematic uncertainty of 3.8 fs. In the fit to the decay time the correlation between the time resolution and its uncertainty is ignored. The possible bias from this assumption is evaluated to be less than 0.3 fs. Varying the time resolution, in the range $40 - 60$ fs, does not change the result and no uncertainty is assigned.

Uncertainties arising from the modelling of the signal and background mass distributions are evaluated using the discrete profiling method described in Ref. [36]. In the default fit the yield of the $B^0 \to J/\psi\eta$ component is left free. Constraining it using the knowledge of the branching fractions in Ref. [5] and the fragmentation fractions given in Ref. [37] changes $\tau_{\rm L}$ by 0.4 fs which is assigned as a systematic.

Further small uncertainties arise from the limited knowledge of the length scale of the detector along the beam axis (z-scale), the momentum scale for charged particles and the neutral particle energy scale. An additional 1 fs systematic uncertainty arises from the effect of B_s^0 mesons produced via B_c^+ decays [38].

The stability of the result is tested by dividing the data according to the year of running (Fig. 3, left), the $p_{\rm T}$ of the B_s^0 candidate (Fig. 3, right) and by varying the requirements on the MVA, the $\chi^2_{\rm IP}$ and the value of the minimum decay time requirement. No significant change in the final result is found and hence no further systematic uncertainty is assigned.

The systematic uncertainties are summarized in Table 1. Adding them in quadrature leads to a total systematic uncertainty of 8.0 fs.

6 Summary

Using the dataset collected by LHCb during Run 2, the effective lifetime in the $B_s^0 \to J/\psi\eta$ decay mode is measured to be

$$\tau_{\rm L} = 1.445 \pm 0.016\,(\text{stat}) \pm 0.008\,(\text{syst})\,\text{ps}.$$

This result agrees with the Run 1 measurement [6] within 1σ

$$\tau_{\rm L} = 1.479 \pm 0.034\,(\text{stat}) \pm 0.011\,(\text{syst})\,\text{ps},$$

and is a factor of two more precise. The two values are combined assuming the uncertainties due to the momentum and length scales, B^0 background, partially reconstructed background, mass model, time resolution and possible B_c^+ component are fully correlated. The remaining systematic uncertainties, dominated by the simulated samples sizes, are taken to be uncorrelated. The combination gives

$$\tau_{\rm L} = 1.452 \pm 0.014 \pm 0.007 \pm 0.002\,\text{ps},$$

where the first uncertainty is statistical, the second is the uncorrelated systematic uncertainty and the third is the correlated systematic uncertainty. This combination supersedes the previous result in the $B_s^0 \to J/\psi\eta$ mode. It is

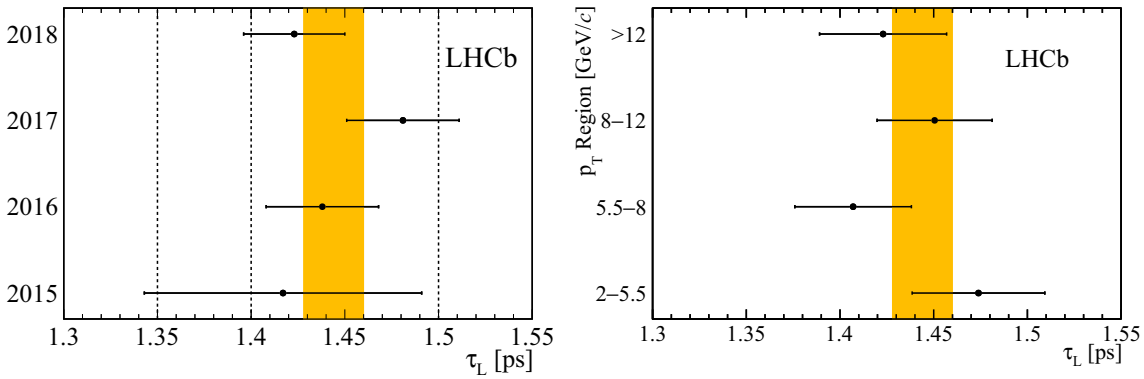

Fig. 3 Values of τ_L obtained by dividing the data according to (left) the four years of data-taking and (right) regions in B_s^0 p_T. In both plots the statistical uncertainty for each point is shown. The 1σ error bands of the statistical uncertainty on the combined results are shown in yellow. The χ^2 probability of the measurements is 51 %(49 %) for fits to the data divided by year (B_s^0 p_T)

Table 1 Systematic uncertainties on the lifetime measurement in fs. Uncertainties less than 0.1 fs are indicated with a dash

Source	Uncertainty [fs]
Simulated sample sizes	5.2
A_{VELO}	1.1
A_{DLS}	–
$A_{\text{IP}\chi^2}$	0.4
A_{MVA}	1.7
B^+ lifetime	4.0
Time resolution model	0.3
VELO half alignment	3.8
τ for $B_s^0 \to \chi_c \eta$ component	0.7
Mass model	0.8
B^0 component	0.4
Momentum scale	–
z-scale	0.3
Data-simulation χ^2_{IP} differences	0.1
Mass-time correlation	0.5
B_c^+ component	1.0
Quadrature sum	8.0

in agreement at 2σ, but more precise than, the measurement made using the $B_s^0 \to D_s^+ D_s^-$ decay mode $\tau_L = 1.379 \pm 0.026\,(\text{stat}) \pm 0.017\,(\text{syst})$ ps [7]. A weighted average of the tree-level measurements gives $\tau_L = 1.437 \pm 0.014$ ps. This agrees at the 1σ level with the Standard Model expectation of $\tau_L = 1.422 \pm 0.013$ ps [1,4]. The result also agrees at the 2σ level with the value quoted by HFLAV [35] based upon measurements of Γ_s and $\Delta\Gamma_s$ in the $B_s^0 \to J/\psi\phi$ decay mode, $\tau_L = 1.426 \pm 0.008$ ps. Finally, it is also consistent with the value of $1.407 \pm 0.016\,(\text{stat}) \pm 0.007\,(\text{syst})$ ps found in the penguin-dominated decay $B_s^0 \to K^+K^-$ [8]. Figure 4 summarizes the measurements of τ_L in all these modes.

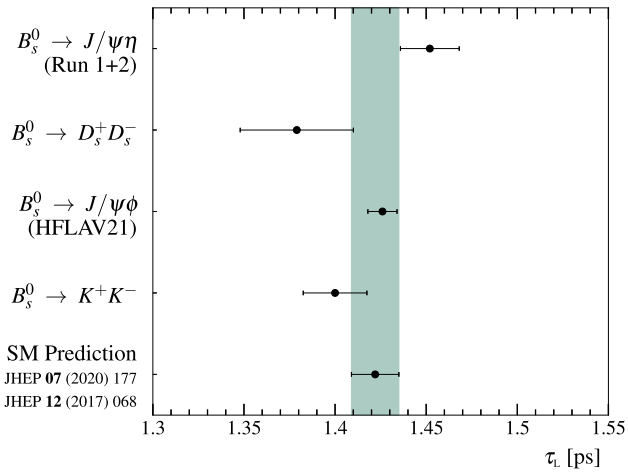

Fig. 4 Summary of measurements of τ_L from LHCb [7,8] along with the HFLAV average [35] determined using the measurements of Γ_s and $\Delta\Gamma_s$ made using the $B_s^0 \to J/\psi\phi$ decay mode. The SM prediction, calculated using the values in Refs. [1,4] is shown by the grey-green band

Further improvements in precision in τ_L are expected both by considering other CP-even B_s^0 decays to final states containing η or η' mesons, the $B_s^0 \to D_s^+ D_s^-$ dataset collected during Run 2 and from the larger dataset that will be collected by the upgraded LHCb detector.

Acknowledgements We express our gratitude to our colleagues in the CERN accelerator departments for the excellent performance of the LHC. We thank the technical and administrative staff at the LHCb institutes. We acknowledge support from CERN and from the national agencies: CAPES, CNPq, FAPERJ and FINEP (Brazil); MOST and NSFC (China); CNRS/IN2P3 (France); BMBF, DFG and MPG (Germany); INFN (Italy); NWO (Netherlands); MNiSW and NCN (Poland); MEN/IFA (Romania); MICINN (Spain); SNSF and SER (Switzerland); NASU (Ukraine); STFC (United Kingdom); DOE NP and NSF (USA). We acknowledge the computing resources that are provided by CERN, IN2P3 (France), KIT and DESY (Germany), INFN (Italy), SURF (Netherlands), PIC (Spain), GridPP (United Kingdom), CSCS

(Switzerland), IFIN-HH (Romania), CBPF (Brazil), Polish WLCG (Poland) and NERSC (USA). We are indebted to the communities behind the multiple open-source software packages on which we depend. Individual groups or members have received support from ARC and ARDC (Australia); Minciencias (Colombia); AvH Foundation (Germany); EPLANET, Marie Skłodowska-Curie Actions and ERC (European Union); A*MIDEX, ANR, IPhU and Labex P2IO, and Région Auvergne-Rhône-Alpes (France); Key Research Program of Frontier Sciences of CAS, CAS PIFI, CAS CCEPP, Fundamental Research Funds for the Central Universities, and Sci. and Tech. Program of Guangzhou (China); GVA, XuntaGal and GENCAT (Spain); SRC (Sweden); the Leverhulme Trust, the Royal Society and UKRI (United Kingdom).

Data Availability Statement This manuscript has associated data in a data repository. [Authors' comment: ...].

Funded by SCOAP[3]. SCOAP[3] supports the goals of the International Year of Basic Sciences for Sustainable Development.

References

1. A. Lenz, G. Tetlalmatzi-Xolocotzi, Model-independent bounds on new physics effects in non-leptonic tree-level decays of B-mesons. JHEP **07**, 177 (2020). https://doi.org/10.1007/JHEP07(2020)177. arXiv:1912.07621
2. R. Fleischer, R. Knegjens, Effective lifetimes of B_s decays and their constraints on the B_s^0-$\bar{B}_s^0$ mixing parameters. Eur. Phys. J. C **71**, 1789 (2011). https://doi.org/10.1140/epjc/s10052-011-1789-9. arXiv:1109.5115
3. R. Fleischer, R. Knegjens, G. Ricciardi, Exploring CP violation and η-η' mixing with the $B_{s,d}^0 \to J/\psi\eta^{(\prime)}$ systems. Eur. Phys. J. C **71**, 1798 (2011). https://doi.org/10.1140/epjc/s10052-011-1798-8. arXiv:1110.5490
4. M. Kirk, A. Lenz, T. Rauh, Dimension-six matrix elements for meson mixing and lifetimes from sum rules. JHEP **12**, 068 (2017). https://doi.org/10.1007/JHEP12(2017)068. arXiv:1711.02100 [Erratum: JHEP **06**, 162 (2020), https://doi.org/10.1007/JHEP06(2020)162]
5. Particle Data Group, P.A. Zyla et al., Review of particle physics. Prog. Theor. Exp. Phys. **2020**, 083C01 (2020). https://doi.org/10.1093/ptep/ptaa104
6. LHCb Collaboration, R. Aaij et al., Measurement of the $B_s^0 \to J/\psi\eta$ lifetime. Phys. Lett. B **762**, 484 (2016). https://doi.org/10.1016/j.physletb.2016.10.006. arXiv:1607.06314
7. LHCb Collaboration, R. Aaij et al., Measurement of the $\bar{B}_s^0 \to D_s^- D_s^+$ and $\bar{B}_s^0 \to D^- D_s^+$ effective lifetimes. Phys. Rev. Lett. **112**, 111802 (2014). https://doi.org/10.1103/PhysRevLett.112.111802. arXiv:1312.1217
8. LHCb Collaboration, R. Aaij et al., Effective lifetime measurements in the $B_s^0 \to K^+K^-$, $B_s^0 \to K^+\pi^-$ *and* $B_s^0 \to \pi^+K^-$ *decays*. Phys. Lett. B **736**, 446 (2014). https://doi.org/10.1016/j.physletb.2014.07.051. arXiv:1406.7204
9. LHCb Collaboration, R. Aaij et al., Measurement of the $\bar{B}_s^0$ effective lifetime in the $J/\psi f_0(980)$ final state. Phys. Rev. Lett. **109**, 152002 (2012). https://doi.org/10.1103/PhysRevLett.109.152002. arXiv:1207.0878
10. D0 Collaboration, V.M. Abazov et al., B_s^0 lifetime measurement in the CP-odd decay channel $B_s^0 \to J/\psi f_0(980)$. Phys. Rev. D **94**, 012001 (2016). https://doi.org/10.1103/PhysRevD.94.012001. arXiv:1603.01302
11. CMS Collaboration, A.M. Sirunyan et al., Measurement of b hadron lifetimes in pp collisions at $\sqrt{s} = 8$ TeV. Eur. Phys. J. C **78**, 457 (2018). https://doi.org/10.1140/epjc/s10052-018-5929-3. arXiv:1710.08949 [Erratum: Eur. Phys. J. C **78**, 561 (2018), https://doi.org/10.1140/epjc/s10052-018-6014-7]
12. A.A. Alves Jr. et al., Performance of the LHCb muon system. JINST **8**, P02022 (2013). https://doi.org/10.1088/1748-0221/8/02/P02022. arXiv:1211.1346
13. LHCb Collaboration, R. Aaij et al., LHCb detector performance. Int. J. Mod. Phys. A **30**, 1530022 (2015). https://doi.org/10.1142/S0217751X15300227. arXiv:1412.6352
14. LHCb Collaboration, R. Aaij et al., Precision measurement of D meson mass differences. JHEP **06**, 065 (2013). https://doi.org/10.1007/JHEP06(2013)065. arXiv:1304.6865
15. C. Abellan Beteta et al., Calibration and performance of the LHCb calorimeters in Run 1 and 2 at the LHC. JINST. arXiv:2008.11556 **(submitted)**
16. R. Aaij et al., Performance of the LHCb trigger and full real-time reconstruction in Run 2 of the LHC. JINST **14**, P04013 (2019). https://doi.org/10.1088/1748-0221/14/04/P04013. arXiv:1812.10790
17. S. Borghi, Novel real-time alignment and calibration of the LHCb detector and its performance. Nucl. Instrum. Meth. A **845**, 560 (2017). https://doi.org/10.1016/j.nima.2016.06.050
18. T. Sjöstrand, S. Mrenna, P. Skands, PYTHIA 6.4 physics and manual. JHEP **05**, 026 (2006). https://doi.org/10.1088/1126-6708/2006/05/026. arXiv:hep-ph/0603175
19. T. Sjöstrand, S. Mrenna, P. Skands, A brief introduction to PYTHIA 8.1. Comput. Phys. Commun. **178**, 852 (2008). https://doi.org/10.1016/j.cpc.2008.01.036. arXiv:0710.3820
20. I. Belyaev et al., Handling of the generation of primary events in Gauss, the LHCb simulation framework. J. Phys. Conf. Ser. **331**, 032047 (2011). https://doi.org/10.1088/1742-6596/331/3/032047
21. D.J. Lange, The EvtGen particle decay simulation package. Nucl. Instrum. Meth. **A462**, 152 (2001). https://doi.org/10.1016/S0168-9002(01)00089-4
22. P. Golonka, Z. Was, PHOTOS Monte Carlo: a precision tool for QED corrections in Z and W decays. Eur. Phys. J. C **45**, 97 (2006). https://doi.org/10.1140/epjc/s2005-02396-4. arXiv:hep-ph/0506026
23. Geant4 Collaboration, J. Allison et al., Geant4 developments and applications. IEEE Trans. Nucl. Sci. **53**, 270 (2006). https://doi.org/10.1109/TNS.2006.869826
24. Geant4 Collaboration, S. Agostinelli et al., Geant4: a simulation toolkit. Nucl. Instrum. Meth. A **506**, 250 (2003). https://doi.org/10.1016/S0168-9002(03)01368-8
25. M. Clemencic et al., The *LHCb* simulation application, Gauss: design, evolution and experience. J. Phys. Conf. Ser. **331**, 032023 (2011). https://doi.org/10.1088/1742-6596/331/3/032023
26. G.A. Cowan, D.C. Craik, M.D. Needham, RapidSim: an application for the fast simulation of heavy-quark hadron decays. Comput. Phys. Commun. **214**, 239 (2017). https://doi.org/10.1016/j.cpc.2017.01.029. arXiv:1612.07489

27. W.D. Hulsbergen, Decay chain fitting with a Kalman filter. Nucl. Instrum. Meth. **A552**, 566 (2005). https://doi.org/10.1016/j.nima.2005.06.078. arXiv:physics/0503191
28. H. Voss, A. Hoecker, J. Stelzer, F. Tegenfeldt, TMVA—toolkit for multivariate data analysis with ROOT. PoS **ACAT**, 040 (2007). https://doi.org/10.22323/1.050.0040
29. M. Pivk, F.R. Le Diberder, sPlot: a statistical tool to unfold data distributions. Nucl. Instrum. Meth. A **555**, 356 (2005). https://doi.org/10.1016/j.nima.2005.08.106. arXiv:physics/0402083
30. LHCb Collaboration, R. Aaij et al., Measurements of the B^+, B^0 B_s^0 meson and Λ_b^0 baryon lifetimes. JHEP **04**, 114 (2014). https://doi.org/10.1007/JHEP04(2014)114. arXiv:1402.2554
31. T. Skwarnicki, A study of the radiative cascade transitions between the Upsilon-prime and Upsilon resonances, PhD thesis (Institute of Nuclear Physics, Krakow, 1986). http://inspirehep.net/record/230779/DESY-F31-86-02
32. BABAR Collaboration, J.P. Lees et al., Branching fraction measurements of the color-suppressed decays $\bar{B}^0 \to D^{(*)0}\pi^0$, $D_\eta^{(*)0}$, $D_\omega^{(*)0}$, and $D_\eta^{(*)0\prime}$ and measurement of the polarization in the decay $\overline{B}^0 \to D_\omega^{*0}$. Phys. Rev. D **84**, 112007 (2011). https://doi.org/10.1103/PhysRevD.84.112007. arXiv:1107.5751 [Erratum: Phys. Rev. D **87**, 039901 (2013), https://doi.org/10.1103/PhysRevD.87.039901]
33. C. Hansen, J.B. McDonald, W.K. Newey, Instrumental variables estimation with flexible distributions. J. Bus. Econ. Stat. **28**, 13 (2010). https://doi.org/10.1198/jbes.2009.06161
34. P. Theodossiou, Financial data and the skewed generalized t distribution. Manag. Sci. **44**, 1650 (1998). https://doi.org/10.1287/mnsc.44.12.1650
35. Heavy Flavor Averaging Group, Y. Amhis et al., Averages of b-hadron, c-hadron, and τ-lepton properties as of 2018. Eur. Phys. J. C **81**, 226 (2021). https://doi.org/10.1140/epjc/s10052-020-8156-7. arXiv:1909.12524 (updated results and plots available at https://hflav.web.cern.ch)
36. P.D. Dauncey, M. Kenzie, N. Wardle, G.J. Davies, Handling uncertainties in background shapes: the discrete profiling method. JINST **10**, P04015 (2015). https://doi.org/10.1088/1748-0221/10/04/P04015. arXiv:1408.6865
37. LHCb Collaboration, R. Aaij et al., Precise measurement of the f_s/f_d ratio of fragmentation fractions and of B_s^0 decay branching fractions. Phys. Rev. D **104**, 032005 (2021). https://doi.org/10.1103/PhysRevD.104.032005. arXiv:2103.06810
38. LHCb Collaboration, R. Aaij et al., Updated measurement of time-dependent CP-violating observables in $B_s^0 \to J/\psi K^+K^-$ *decays*. Eur. Phys. J. C **79**, 706 (2019). https://doi.org/10.1140/epjc/s10052-019-7159-8. arXiv:1906.08356 [Erratum: Eur. Phys. J. C **80**, 601 (2020), https://doi.org/10.1140/epjc/s10052-020-7875-0]

LHCb collaboration*

R. Aaij[32], A. S. W. Abdelmotteleb[50], C. Abellan Beteta[44], F. Abudinén[50], T. Ackernley[54], B. Adeva[40], M. Adinolfi[48], H. Afsharnia[9], C. Agapopoulou[13], C. A. Aidala[76], S. Aiola[25], Z. Ajaltouni[9], S. Akar[59], K. Akiba[32], J. Albrecht[15], F. Alessio[42], M. Alexander[53], A. Alfonso Albero[39], Z. Aliouche[56], P. Alvarez Cartelle[49], R. Amalric[13], S. Amato[2], J. L. Amey[48], Y. Amhis[11,42], L. An[42], L. Anderlini[22], M. Andersson[44], A. Andreianov[38], M. Andreotti[21], D. Andreou[62], D. Ao[6], F. Archilli[17], A. Artamonov[38], M. Artuso[62], E. Aslanides[10], M. Atzeni[44], B. Audurier[12], S. Bachmann[17], M. Bachmayer[43], J. J. Back[50], A. Bailly-reyre[13], P. Baladron Rodriguez[40], V. Balagura[12], W. Baldini[21], J. Baptista de Souza Leite[1], M. Barbetti[22,j], R. J. Barlow[56], S. Barsuk[11], W. Barter[55], M. Bartolini[49], F. Baryshnikov[38], J. M. Basels[14], G. Bassi[29,q], B. Batsukh[4], A. Battig[15], A. Bay[43], A. Beck[50], M. Becker[15], F. Bedeschi[29], I. B. Bediaga[1], A. Beiter[62], V. Belavin[38], S. Belin[40], V. Bellee[44], K. Belous[38], I. Belov[38], I. Belyaev[38], G. Bencivenni[23], E. Ben-Haim[13], A. Berezhnoy[38], R. Bernet[44], D. Berninghoff[17], H. C. Bernstein[62], C. Bertella[56], A. Bertolin[28], C. Betancourt[44], F. Betti[42], Ia. Bezshyiko[44], S. Bhasin[48], J. Bhom[35], L. Bian[67], M. S. Bieker[15], N. V. Biesuz[21], S. Bifani[47], P. Billoir[13], A. Biolchini[32], M. Birch[55], F. C. R. Bishop[49], A. Bitadze[56], A. Bizzeti, M. P. Blago[49], T. Blake[50], F. Blanc[43], S. Blusk[62], D. Bobulska[53], J. A. Boelhauve[15], O. Boente Garcia[12], T. Boettcher[59], A. Boldyrev[38], C. S. Bolognani[73], N. Bondar[38,42], S. Borghi[56], M. Borsato[17], J. T. Borsuk[35], S. A. Bouchiba[43], T. J. V. Bowcock[42,54], A. Boyer[42], C. Bozzi[21], M. J. Bradley[55], S. Braun[60], A. Brea Rodriguez[40], J. Brodzicka[35], A. Brossa Gonzalo[50], D. Brundu[27], A. Buonaura[44], L. Buonincontri[28], A. T. Burke[56], C. Burr[42], A. Bursche[66], A. Butkevich[38], J. S. Butter[32], J. Buytaert[42], W. Byczynski[42], S. Cadeddu[27], H. Cai[67], R. Calabrese[21,i], L. Calefice[13,15], S. Cali[23], R. Calladine[47], M. Calvi[26,m], M. Calvo Gomez[74], P. Camargo Magalhaes[48], P. Campana[23], D. H. Campora Perez[73], A. F. Campoverde Quezada[6], S. Capelli[26,m], L. Capriotti[20,g], A. Carbone[20,g], G. Carboni[31], R. Cardinale[24,k], A. Cardini[27], I. Carli[4], P. Carniti[26,m], L. Carus[14], A. Casais Vidal[40], R. Caspary[17], G. Casse[54], M. Cattaneo[42], G. Cavallero[42], V. Cavallini[21,i], S. Celani[43], J. Cerasoli[10], D. Cervenkov[57], A. J. Chadwick[54], M. G. Chapman[48], M. Charles[13], Ph. Charpentier[42], C. A. Chavez Barajas[54], M. Chefdeville[8], C. Chen[3], S. Chen[4], A. Chernov[35], S. Chernyshenko[46], V. Chobanova[40], S. Cholak[43], M. Chrzaszcz[35], A. Chubykin[38], V. Chulikov[38], P. Ciambrone[23], M. F. Cicala[50], X. Cid Vidal[40], G. Ciezarek[42], G. Ciullo[21,i], P. E. L. Clarke[52], M. Clemencic[42], H. V. Cliff[49], J. Closier[42], J. L. Cobbledick[56], V. Coco[42], J. A. B. Coelho[11], J. Cogan[10], E. Cogneras[9], L. Cojocariu[37], P. Collins[42],

T. Colombo[42], L. Congedo[19], A. Contu[27], N. Cooke[47], G. Coombs[53], I. Corredoira[40], G. Corti[42], B. Couturier[42], D. C. Craik[58], J. Crkovská[61], M. Cruz Torres[1,e], R. Currie[52], C. L. Da Silva[61], S. Dadabaev[38], L. Dai[65], E. Dall'Occo[15], J. Dalseno[40], C. D'Ambrosio[42], A. Danilina[38], P. d'Argent[15], J. E. Davies[56], A. Davis[56], O. De Aguiar Francisco[56], J. de Boer[42], K. De Bruyn[72], S. De Capua[56], M. De Cian[43], U. De Freitas Carneiro Da Graca[1], E. De Lucia[23], J. M. De Miranda[1], L. De Paula[2], M. De Serio[19,f], D. De Simone[44], P. De Simone[23], F. De Vellis[15], J. A. de Vries[73], C. T. Dean[61], F. Debernardis[19,f], D. Decamp[8], V. Dedu[10], L. Del Buono[13], B. Delaney[58], H.-P. Dembinski[15], V. Denysenko[44], O. Deschamps[9], F. Dettori[27,h], B. Dey[70], A. Di Cicco[23], P. Di Nezza[23], I. Diachkov[38], S. Didenko[38], L. Dieste Maronas[40], S. Ding[62], V. Dobishuk[46], A. Dolmatov[38], C. Dong[3], A. M. Donohoe[18], F. Dordei[27], A. C. dos Reis[1], L. Douglas[53], A. G. Downes[8], M. W. Dudek[35], L. Dufour[42], V. Duk[71], P. Durante[42], J. M. Durham[61], D. Dutta[56], A. Dziurda[35], A. Dzyuba[38], S. Easo[51], U. Egede[63], V. Egorychev[38], S. Eidelman[38,*], S. Eisenhardt[52], S. Ek-In[43], L. Eklund[75], S. Ely[62], A. Ene[37], E. Epple[61], S. Escher[14], J. Eschle[44], S. Esen[44], T. Evans[56], L. N. Falcao[1], Y. Fan[6], B. Fang[67], S. Farry[54], D. Fazzini[26,m], M. Feo[42], A. D. Fernez[60], F. Ferrari[20], L. Ferreira Lopes[43], F. Ferreira Rodrigues[2], S. Ferreres Sole[32], M. Ferrillo[44], M. Ferro-Luzzi[42], S. Filippov[38], R. A. Fini[19], M. Fiorini[21,i], M. Firlej[34], K. M. Fischer[57], D. S. Fitzgerald[76], C. Fitzpatrick[56], T. Fiutowski[34], F. Fleuret[12], M. Fontana[13], F. Fontanelli[24,k], R. Forty[42], D. Foulds-Holt[49], V. Franco Lima[54], M. Franco Sevilla[60], M. Frank[42], E. Franzoso[21,i], G. Frau[17], C. Frei[42], D. A. Friday[53], J. Fu[6], Q. Fuehring[15], E. Gabriel[32], G. Galati[19,f], M. D. Galati[72], A. Gallas Torreira[40], D. Galli[20,g], S. Gambetta[42,52], Y. Gan[3], M. Gandelman[2], P. Gandini[25], Y. Gao[5], M. Garau[27,h], L. M. Garcia Martin[50], P. Garcia Moreno[39], J. García Pardiñas[26,m], B. Garcia Plana[40], F. A. Garcia Rosales[12], L. Garrido[39], C. Gaspar[42], R. E. Geertsema[32], D. Gerick[17], L. L. Gerken[15], E. Gersabeck[56], M. Gersabeck[56], T. Gershon[50], L. Giambastiani[28], V. Gibson[49], H. K. Giemza[36], A. L. Gilman[57], M. Giovannetti[23,t], A. Gioventù[40], P. Gironella Gironell[39], C. Giugliano[21,i], M. A. Giza[35], K. Gizdov[52], E. L. Gkougkousis[42], V. V. Gligorov[13,42], C. Göbel[64], E. Golobardes[74], D. Golubkov[38], A. Golutvin[38,55], A. Gomes[1,a], S. Gomez Fernandez[39], F. Goncalves Abrantes[57], M. Goncerz[35], G. Gong[3], I. V. Gorelov[38], C. Gotti[26], J. P. Grabowski[17], T. Grammatico[13], L. A. Granado Cardoso[42], E. Graugés[39], E. Graverini[43], G. Graziani, A. T. Grecu[37], L. M. Greeven[32], N. A. Grieser[4], L. Grillo[53], S. Gromov[38], B. R. Gruberg Cazon[57], C. Gu[3], M. Guarise[21,i], M. Guittiere[11], P. A. Günther[17], E. Gushchin[38], A. Guth[14], Y. Guz[38], T. Gys[42], T. Hadavizadeh[63], G. Haefeli[43], C. Haen[42], J. Haimberger[42], S. C. Haines[49], T. Halewood-leagas[54], M. M. Halvorsen[42], P. M. Hamilton[60], J. Hammerich[54], Q. Han[7], X. Han[17], E. B. Hansen[56], S. Hansmann-Menzemer[17,42], L. Hao[6], N. Harnew[57], T. Harrison[54], C. Hasse[42], M. Hatch[42], J. He[6,c], K. Heijhoff[32], K. Heinicke[15], R. D. L. Henderson[50,63], A. M. Hennequin[58], K. Hennessy[54], L. Henry[42], J. Heuel[14], A. Hicheur[2], D. Hill[43], M. Hilton[56], S. E. Hollitt[15], R. Hou[7], Y. Hou[8], J. Hu[17], J. Hu[66], W. Hu[5], X. Hu[3], W. Huang[6], X. Huang[67], W. Hulsbergen[32], R. J. Hunter[50], M. Hushchyn[38], D. Hutchcroft[54], P. Ibis[15], M. Idzik[34], D. Ilin[38], P. Ilten[59], A. Inglessi[38], A. Iniukhin[38], A. Ishteev[38], K. Ivshin[38], R. Jacobsson[42], H. Jage[14], S. J. Jaimes Elles[41], S. Jakobsen[42], E. Jans[32], B. K. Jashal[41], A. Jawahery[60], V. Jevtic[15], X. Jiang[4,6], Y. Jiang[6], M. John[57], D. Johnson[58], C. R. Jones[49], T. P. Jones[50], B. Jost[42], N. Jurik[42], I. Juszczak[35], S. Kandybei[45], Y. Kang[3], M. Karacson[42], D. Karpenkov[38], M. Karpov[38], J. W. Kautz[59], F. Keizer[42], D. M. Keller[62], M. Kenzie[50], T. Ketel[33], B. Khanji[15], A. Kharisova[38], S. Kholodenko[38], T. Kirn[14], V. S. Kirsebom[43], O. Kitouni[58], S. Klaver[33], N. Kleijne[29,q], K. Klimaszewski[36], M. R. Kmiec[36], S. Koliiev[46], A. Kondybayeva[38], A. Konoplyannikov[38], P. Kopciewicz[34], R. Kopecna[17], P. Koppenburg[32], M. Korolev[38], I. Kostiuk[32,46], O. Kot[46], S. Kotriakhova, A. Kozachuk[38], P. Kravchenko[38], L. Kravchuk[38], R. D. Krawczyk[42], M. Kreps[50], S. Kretzschmar[14], P. Krokovny[38], W. Krupa[34], W. Krzemien[36], J. Kubat[17], W. Kucewicz[35,34], M. Kucharczyk[35], V. Kudryavtsev[38], G. J. Kunde[61], D. Lacarrere[42], G. Lafferty[56], A. Lai[27], A. Lampis[27,h], D. Lancierini[44], J. J. Lane[56], R. Lane[48], G. Lanfranchi[23], C. Langenbruch[14], J. Langer[15], O. Lantwin[38], T. Latham[50], F. Lazzari[29,u], M. Lazzaroni[25,l], R. Le Gac[10], S. H. Lee[76], R. Lefèvre[9], A. Leflat[38], S. Legotin[38], P. Lenisa[21,i], O. Leroy[10], T. Lesiak[35], B. Leverington[17], H. Li[66], K. Li[7], P. Li[17], S. Li[7], T. Li[66], Y. Li[4], Z. Li[62], X. Liang[62], C. Lin[6], T. Lin[51], R. Lindner[42], V. Lisovskyi[15], R. Litvinov[27,h], G. Liu[66], H. Liu[6], Q. Liu[6], S. Liu[4,6], A. Lobo Salvia[39], A. Loi[27], R. Lollini[71], J. Lomba Castro[40], I. Longstaff[53], J. H. Lopes[2], S. López Soliño[40], G. H. Lovell[49], Y. Lu[4,b], C. Lucarelli[22,j], D. Lucchesi[28,o], S. Luchuk[38], M. Lucio Martinez[32], V. Lukashenko[32,46], Y. Luo[3], A. Lupato[56], E. Luppi[21,i], A. Lusiani[29,q], K. Lynch[18], X.-R. Lyu[6], L. Ma[4], R. Ma[6], S. Maccolini[20], F. Machefert[11], F. Maciuc[37], I. Mackay[57], V. Macko[43], P. Mackowiak[15],

S. Maddrell-Mander[48], L. R. Madhan Mohan[48], A. Maevskiy[38], D. Maisuzenko[38], M. W. Majewski[34], J. J. Malczewski[35], S. Malde[57], B. Malecki[35,42], A. Malinin[38], T. Maltsev[38], H. Malygina[17], G. Manca[27,h], G. Mancinelli[10], D. Manuzzi[20], C. A. Manzari[44], D. Marangotto[25,l], J. F. Marchand[8], U. Marconi[20], S. Mariani[22,j], C. Marin Benito[39], M. Marinangeli[43], J. Marks[17], A. M. Marshall[48], P. J. Marshall[54], G. Martelli[71,p], G. Martellotti[30], L. Martinazzoli[42,m], M. Martinelli[26,m], D. Martinez Santos[40], F. Martinez Vidal[41], A. Massafferri[1], M. Materok[14], R. Matev[42], A. Mathad[44], V. Matiunin[38], C. Matteuzzi[26], K. R. Mattioli[76], A. Mauri[32], E. Maurice[12], J. Mauricio[39], M. Mazurek[42], M. McCann[55], L. Mcconnell[18], T. H. McGrath[56], N. T. McHugh[53], A. McNab[56], R. McNulty[18], J. V. Mead[54], B. Meadows[59], G. Meier[15], D. Melnychuk[36], S. Meloni[26,m], M. Merk[32,73], A. Merli[25,l], L. Meyer Garcia[2], D. Miao[4,6], M. Mikhasenko[69,d], D. A. Milanes[68], E. Millard[50], M. Milovanovic[42], M.-N. Minard[8,*], A. Minotti[26,m], S. E. Mitchell[52], B. Mitreska[56], D. S. Mitzel[15], A. Mödden[15], R. A. Mohammed[57], R. D. Moise[55], S. Mokhnenko[38], T. Mombächer[40], I. A. Monroy[68], S. Monteil[9], M. Morandin[28], G. Morello[23], M. J. Morello[29,q], J. Moron[34], A. B. Morris[69], A. G. Morris[50], R. Mountain[62], H. Mu[3], F. Muheim[52], M. Mulder[72], K. Müller[44], C. H. Murphy[57], D. Murray[56], R. Murta[55], P. Muzzetto[27,h], P. Naik[48], T. Nakada[43], R. Nandakumar[51], T. Nanut[42], I. Nasteva[2], M. Needham[52], N. Neri[25,l], S. Neubert[69], N. Neufeld[42], P. Neustroev[38], R. Newcombe[55], E. M. Niel[43], S. Nieswand[14], N. Nikitin[38], N. S. Nolte[58], C. Normand[8,h,27], C. Nunez[76], A. Oblakowska-Mucha[34], V. Obraztsov[38], T. Oeser[14], D. P. O'Hanlon[48], S. Okamura[21,i], R. Oldeman[27,h], F. Oliva[52], M. E. Olivares[62], C. J. G. Onderwater[72], R. H. O'Neil[52], J. M. Otalora Goicochea[2], T. Ovsiannikova[38], P. Owen[44], A. Oyanguren[41], O. Ozcelik[52], K. O. Padeken[69], B. Pagare[50], P. R. Pais[42], T. Pajero[57], A. Palano[19], M. Palutan[23], Y. Pan[56], G. Panshin[38], A. Papanestis[51], M. Pappagallo[19,f], L. L. Pappalardo[21,i], C. Pappenheimer[59], W. Parker[60], C. Parkes[56], B. Passalacqua[21,i], G. Passaleva[22], A. Pastore[19], M. Patel[55], C. Patrignani[20,g], C. J. Pawley[73], A. Pearce[42], A. Pellegrino[32], M. Pepe Altarelli[42], S. Perazzini[20], D. Pereima[38], A. Pereiro Castro[40], P. Perret[9], M. Petric[53], K. Petridis[48], A. Petrolini[24,k], A. Petrov[38], S. Petrucci[52], M. Petruzzo[25], H. Pham[62], A. Philippov[38], R. Piandani[6], L. Pica[29,q], M. Piccini[71], B. Pietrzyk[8], G. Pietrzyk[11], M. Pili[57], D. Pinci[30], F. Pisani[42], M. Pizzichemi[26,m,42], V. Placinta[37], J. Plews[47], M. Plo Casasus[40], F. Polci[13,42], M. Poli Lener[23], M. Poliakova[62], A. Poluektov[10], N. Polukhina[38], I. Polyakov[42], E. Polycarpo[2], S. Ponce[42], D. Popov[6,42], S. Popov[38], S. Poslavskii[38], K. Prasanth[35], L. Promberger[42], C. Prouve[40], V. Pugatch[46], V. Puill[11], G. Punzi[29,r], H. R. Qi[3], W. Qian[6], N. Qin[3], S. Qu[3], R. Quagliani[43], N. V. Raab[18], R. I. Rabadan Trejo[6], B. Rachwal[34], J. H. Rademacker[48], R. Rajagopalan[62], M. Rama[29], M. Ramos Pernas[50], M. S. Rangel[2], F. Ratnikov[38], G. Raven[33,42], M. Rebollo De Miguel[41], F. Redi[42], F. Reiss[56], C. Remon Alepuz[41], Z. Ren[3], V. Renaudin[57], P. K. Resmi[10], R. Ribatti[29,q], A. M. Ricci[27], S. Ricciardi[51], K. Rinnert[54], P. Robbe[11], G. Robertson[52], A. B. Rodrigues[43], E. Rodrigues[54], J. A. Rodriguez Lopez[68], E. Rodriguez Rodriguez[40], A. Rollings[57], P. Roloff[42], V. Romanovskiy[38], M. Romero Lamas[40], A. Romero Vidal[40], J. D. Roth[76,*], M. Rotondo[23], M. S. Rudolph[62], T. Ruf[42], R. A. Ruiz Fernandez[40], J. Ruiz Vidal[41], A. Ryzhikov[38], J. Ryzka[34], J. J. Saborido Silva[40], N. Sagidova[38], N. Sahoo[47], B. Saitta[27,h], M. Salomoni[42], C. Sanchez Gras[32], I. Sanderswood[41], R. Santacesaria[30], C. Santamarina Rios[40], M. Santimaria[23], E. Santovetti[31,t], D. Saranin[38], G. Sarpis[14], M. Sarpis[69], A. Sarti[30], C. Satriano[30,s], A. Satta[31], M. Saur[15], D. Savrina[38], H. Sazak[9], L. G. Scantlebury Smead[57], A. Scarabotto[13], S. Schael[14], S. Scherl[54], M. Schiller[53], H. Schindler[42], M. Schmelling[16], B. Schmidt[42], S. Schmitt[14], O. Schneider[43], A. Schopper[42], M. Schubiger[32], S. Schulte[43], M. H. Schune[11], R. Schwemmer[42], B. Sciascia[23,42], A. Sciuccati[42], S. Sellam[40], A. Semennikov[38], M. Senghi Soares[33], A. Sergi[24,k], N. Serra[44], L. Sestini[28], A. Seuthe[15], Y. Shang[5], D. M. Shangase[76], M. Shapkin[38], I. Shchemerov[38], L. Shchutska[43], T. Shears[54], L. Shekhtman[38], Z. Shen[5], S. Sheng[4,6], V. Shevchenko[38], B. Shi[6], E. B. Shields[26,m], Y. Shimizu[11], E. Shmanin[38], J. D. Shupperd[62], B. G. Siddi[21,i], R. Silva Coutinho[44], G. Simi[28], S. Simone[19,f], M. Singla[63], N. Skidmore[56], R. Skuza[17], T. Skwarnicki[62], M. W. Slater[47], I. Slazyk[21,i], J. C. Smallwood[57], J. G. Smeaton[49], E. Smith[44], M. Smith[55], A. Snoch[32], L. Soares Lavra[9], M. D. Sokoloff[59], F. J. P. Soler[53], A. Solomin[38,48], A. Solovev[38], I. Solovyev[38], F. L. Souza De Almeida[2], B. Souza De Paula[2], B. Spaan[15,*], E. Spadaro Norella[25,l], E. Spiridenkov[38], P. Spradlin[53], V. Sriskaran[42], F. Stagni[42], M. Stahl[59], S. Stahl[42], S. Stanislaus[57], E. N. Stein[42], O. Steinkamp[44], O. Stenyakin[38], H. Stevens[15], S. Stone[62,*], D. Strekalina[38], F. Suljik[57], J. Sun[27], L. Sun[67], Y. Sun[60], P. Svihra[56], P. N. Swallow[47], K. Swientek[34], A. Szabelski[36], T. Szumlak[34], M. Szymanski[42], Y. Tan[3], S. Taneja[56], A. R. Tanner[48], M. D. Tat[57], A. Terentev[38], F. Teubert[42], E. Thomas[42], D. J. D. Thompson[47], K. A. Thomson[54], H. Tilquin[55], V. Tisserand[9], S. T'Jampens[8],

M. Tobin[4], L. Tomassetti[21,i], G. Tonani[25,l], X. Tong[5], D. Torres Machado[1], D. Y. Tou[3], E. Trifonova[38], S. M. Trilov[48], C. Trippl[43], G. Tuci[6], A. Tully[43], N. Tuning[32,42], A. Ukleja[36], D. J. Unverzagt[17], E. Ursov[38], A. Usachov[32], A. Ustyuzhanin[38], U. Uwer[17], A. Vagner[38], V. Vagnoni[20], A. Valassi[42], G. Valenti[20], N. Valls Canudas[74], M. van Beuzekom[32], M. Van Dijk[43], H. Van Hecke[61], E. van Herwijnen[38], M. van Veghel[72], R. Vazquez Gomez[39], P. Vazquez Regueiro[40], C. Vázquez Sierra[42], S. Vecchi[21], J. J. Velthuis[48], M. Veltri[22,v], A. Venkateswaran[62], M. Veronesi[32], M. Vesterinen[50], D. Vieira[59], M. Vieites Diaz[43], X. Vilasis-Cardona[74], E. Vilella Figueras[54], A. Villa[20], P. Vincent[13], F. C. Volle[11], D. vom Bruch[10], A. Vorobyev[38], V. Vorobyev[38], N. Voropaev[38], K. Vos[73], R. Waldi[17], J. Walsh[29], G. Wan[5], C. Wang[17], J. Wang[5], J. Wang[4], J. Wang[3], J. Wang[67], M. Wang[5], R. Wang[48], X. Wang[66], Y. Wang[7], Z. Wang[44], Z. Wang[3], Z. Wang[6], J. A. Ward[50,63], N. K. Watson[47], D. Websdale[55], C. Weisser[58], B. D. C. Westhenry[48], D. J. White[56], M. Whitehead[53], A. R. Wiederhold[50], D. Wiedner[15], G. Wilkinson[57], M. K. Wilkinson[59], I. Williams[49], M. Williams[58], M. R. J. Williams[52], R. Williams[49], F. F. Wilson[51], W. Wislicki[36], M. Witek[35], L. Witola[17], C. P. Wong[61], G. Wormser[11], S. A. Wotton[49], H. Wu[62], K. Wyllie[42], Z. Xiang[6], D. Xiao[7], Y. Xie[7], A. Xu[5], J. Xu[6], L. Xu[3], M. Xu[50], Q. Xu[6], Z. Xu[9], Z. Xu[6], D. Yang[3], S. Yang[6], Y. Yang[6], Z. Yang[5], Z. Yang[60], L. E. Yeomans[54], H. Yin[7], J. Yu[65], X. Yuan[62], E. Zaffaroni[43], M. Zavertyaev[16], M. Zdybal[35], O. Zenaiev[42], M. Zeng[3], D. Zhang[7], L. Zhang[3], S. Zhang[65], S. Zhang[5], Y. Zhang[5], Y. Zhang[57], A. Zharkova[38], A. Zhelezov[17], Y. Zheng[6], T. Zhou[5], X. Zhou[6], Y. Zhou[6], V. Zhovkovska[11], X. Zhu[3], X. Zhu[7], Z. Zhu[6], V. Zhukov[14,38], Q. Zou[4,6], S. Zucchelli[20,g], D. Zuliani[28], G. Zunica[56]

[1] Centro Brasileiro de Pesquisas Físicas (CBPF), Rio de Janeiro, Brazil
[2] Universidade Federal do Rio de Janeiro (UFRJ), Rio de Janeiro, Brazil
[3] Center for High Energy Physics, Tsinghua University, Beijing, China
[4] Institute of High Energy Physics (IHEP), Beijing, China
[5] School of Physics State Key Laboratory of Nuclear Physics and Technology, Peking University, Beijing, China
[6] University of Chinese Academy of Sciences, Beijing, China
[7] Institute of Particle Physics, Central China Normal University, Wuhan, Hubei, China
[8] Université Savoie Mont Blanc, CNRS, IN2P3-LAPP, Annecy, France
[9] Université Clermont Auvergne, CNRS/IN2P3, LPC, Clermont-Ferrand, France
[10] Aix Marseille Univ, CNRS/IN2P3, CPPM, Marseille, France
[11] Université Paris-Saclay, CNRS/IN2P3, IJCLab, Orsay, France
[12] Laboratoire Leprince-Ringuet, CNRS/IN2P3, Ecole Polytechnique, Institut Polytechnique de Paris, Palaiseau, France
[13] LPNHE, Sorbonne Université, Paris Diderot Sorbonne Paris Cité, CNRS/IN2P3, Paris, France
[14] I. Physikalisches Institut, RWTH Aachen University, Aachen, Germany
[15] Fakultät Physik, Technische Universität Dortmund, Dortmund, Germany
[16] Max-Planck-Institut für Kernphysik (MPIK), Heidelberg, Germany
[17] Physikalisches Institut, Ruprecht-Karls-Universität Heidelberg, Heidelberg, Germany
[18] School of Physics, University College Dublin, Dublin, Ireland
[19] INFN Sezione di Bari, Bari, Italy
[20] INFN Sezione di Bologna, Bologna, Italy
[21] INFN Sezione di Ferrara, Ferrara, Italy
[22] INFN Sezione di Firenze, Florence, Italy
[23] INFN Laboratori Nazionali di Frascati, Frascati, Italy
[24] INFN Sezione di Genova, Genoa, Italy
[25] INFN Sezione di Milano, Milan, Italy
[26] INFN Sezione di Milano-Bicocca, Milan, Italy
[27] INFN Sezione di Cagliari, Monserrato, Italy
[28] Università degli Studi di Padova, Università e INFN, Padua, Italy
[29] INFN Sezione di Pisa, Pisa, Italy
[30] INFN Sezione di Roma La Sapienza, Rome, Italy
[31] INFN Sezione di Roma Tor Vergata, Rome, Italy
[32] Nikhef National Institute for Subatomic Physics, Amsterdam, The Netherlands
[33] Nikhef National Institute for Subatomic Physics and VU University Amsterdam, Amsterdam, The Netherlands

[34] Faculty of Physics and Applied Computer Science, AGH-University of Science and Technology, Kraków, Poland
[35] Henryk Niewodniczanski Institute of Nuclear Physics, Polish Academy of Sciences, Kraków, Poland
[36] National Center for Nuclear Research (NCBJ), Warsaw, Poland
[37] Horia Hulubei National Institute of Physics and Nuclear Engineering, Bucharest-Magurele, Romania
[38] Affiliated with an Institute covered by a cooperation agreement with CERN, Geneva, Switzerland
[39] ICCUB, Universitat de Barcelona, Barcelona, Spain
[40] Instituto Galego de Física de Altas Enerxías (IGFAE), Universidade de Santiago de Compostela, Santiago de Compostela, Spain
[41] Instituto de Fisica Corpuscular, Centro Mixto Universidad de Valencia-CSIC, Valencia, Spain
[42] European Organization for Nuclear Research (CERN), Geneva, Switzerland
[43] Institute of Physics, Ecole Polytechnique Fédérale de Lausanne (EPFL), Lausanne, Switzerland
[44] Physik-Institut, Universität Zürich, Zürich, Switzerland
[45] NSC Kharkiv Institute of Physics and Technology (NSC KIPT), Kharkiv, Ukraine
[46] Institute for Nuclear Research of the National Academy of Sciences (KINR), Kyiv, Ukraine
[47] University of Birmingham, Birmingham, UK
[48] H.H. Wills Physics Laboratory, University of Bristol, Bristol, UK
[49] Cavendish Laboratory, University of Cambridge, Cambridge, UK
[50] Department of Physics, University of Warwick, Coventry, UK
[51] STFC Rutherford Appleton Laboratory, Didcot, UK
[52] School of Physics and Astronomy, University of Edinburgh, Edinburgh, UK
[53] School of Physics and Astronomy, University of Glasgow, Glasgow, UK
[54] Oliver Lodge Laboratory, University of Liverpool, Liverpool, UK
[55] Imperial College London, London, UK
[56] Department of Physics and Astronomy, University of Manchester, Manchester, UK
[57] Department of Physics, University of Oxford, Oxford, UK
[58] Massachusetts Institute of Technology, Cambridge, MA, USA
[59] University of Cincinnati, Cincinnati, OH, USA
[60] University of Maryland, College Park, MD, USA
[61] Los Alamos National Laboratory (LANL), Los Alamos, NM, USA
[62] Syracuse University, Syracuse, NY, USA
[63] School of Physics and Astronomy, Monash University, Melbourne, Australia, associated to[50]
[64] Pontifícia Universidade Católica do Rio de Janeiro (PUC-Rio), Rio de Janeiro, Brazil, associated to[2]
[65] Physics and Micro Electronic College, Hunan University, Changsha, China, associated to[7]
[66] Guangdong Provincial Key Laboratory of Nuclear Science, Guangdong-Hong Kong Joint Laboratory of Quantum Matter, Institute of Quantum Matter, South China Normal University, Guangzhou, China, associated to[3]
[67] School of Physics and Technology, Wuhan University, Wuhan, China, associated to[3]
[68] Departamento de Fisica , Universidad Nacional de Colombia, Bogota, Colombia, associated to[13]
[69] Universität Bonn-Helmholtz-Institut für Strahlen und Kernphysik, Bonn, Germany, associated to[17]
[70] Eotvos Lorand University, Budapest, Hungary, associated to[42]
[71] INFN Sezione di Perugia, Perugia, Italy, associated to[21]
[72] Van Swinderen Institute, University of Groningen, Groningen, The Netherlands, associated to[32]
[73] Universiteit Maastricht, Maastricht, The Netherlands associated to[32]
[74] DS4DS, La Salle, Universitat Ramon Llull, Barcelona, Spain, associated to[39]
[75] Department of Physics and Astronomy, Uppsala University, Uppsala, Sweden, associated to[53]
[76] University of Michigan, Ann Arbor, MI, USA, associated to[62]

[a] Universidade Federal do Triângulo Mineiro (UFTM), Uberaba-MG, Brazil
[b] Central South University, Changsha, China
[c] Hangzhou Institute for Advanced Study, UCAS, Hangzhou, China
[d] Excellence Cluster ORIGINS, Munich, Germany
[e] Universidad Nacional Autónoma de Honduras, Tegucigalpa, Honduras
[f] Università di Bari, Bari, Italy
[g] Università di Bologna, Bologna, Italy

[h] Università di Cagliari, Cagliari, Italy
[i] Università di Ferrara, Ferrara, Italy
[j] Università di Firenze, Florence, Italy
[k] Università di Genova, Genoa, Italy
[l] Università degli Studi di Milano, Milan, Italy
[m] Università di Milano Bicocca, Milan, Italy
[n] Università di Modena e Reggio Emilia, Modena, Italy
[o] Università di Padova, Padua, Italy
[p] Università di Perugia, Perugia, Italy
[q] Scuola Normale Superiore, Pisa, Italy
[r] Università di Pisa, Pisa, Italy
[s] Università della Basilicata, Potenza, Italy
[t] Università di Roma Tor Vergata, Rome, Italy
[u] Università di Siena, Siena, Italy
[v] Università di Urbino, Urbino, Italy
[*] Deceased